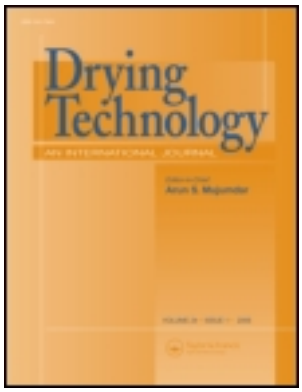

Drying Technology: An International Journal
Publication details, including instructions for authors and subscription information:
http://www.tandfonline.com/loi/ldrt20

A Theoretical Model for the Nongray Radiation Drying of Polyvinylalcohol/Water Solutions

Jyh Jian Chen Ph.D [a] & Jenn Der Lin [b]

[a] Research & Development Division , Precision Instrument Development Center , National Science Council, The Executive Yuan , Hsinchu, Taiwan, R.O.C.

[b] Department of Mechanical Engineering , National Chiao Tung University , Hsinchu, Taiwan, R.O.C.

Published online: 06 Feb 2007.

To cite this article: Jyh Jian Chen Ph.D & Jenn Der Lin (2004) A Theoretical Model for the Nongray Radiation Drying of Polyvinylalcohol/Water Solutions, Drying Technology: An International Journal, 22:4, 853-875, DOI: 10.1081/DRT-120034267

To link to this article: http://dx.doi.org/10.1081/DRT-120034267

DRYING TECHNOLOGY
Vol. 22, No. 4, pp. 853–875, 2004

A Theoretical Model for the Nongray Radiation Drying of Polyvinylalcohol/Water Solutions

Jyh Jian Chen[1,*] and Jenn Der Lin[2]

[1]Research & Development Division, Precision Instrument Development Center, National Science Council, The Executive Yuan, Hsinchu, Taiwan, R.O.C.
[2]Department of Mechanical Engineering, National Chiao Tung University, Hsinchu, Taiwan, R.O.C.

ABSTRACT

A theoretical analysis of heat transfer and moisture variation was performed while a PVA solution was exposed to high-intensity nongray irradiation and/or air flow convection. Effective absorption coefficients were incorporated in the radiative transfer analysis. The influence of various radiation and convection parameters on the transfer of heat and moisture variation in the coated layers on an optically thick substrate was investigated. The effects of radiation and convection parameters on the transfer process were presented

*Correspondence: Jyh Jian Chen, Ph.D, Engineer, Electronics Research & Service Organization, Industrial Technology Research Institute, 195 Sec. 4, Chung Hsing Rd., Chutung, Hsinchu 310, Taiwan, R.O.C; Fax: 886-3-5820266; E-mail: Chaucer@itri.org.tw.

DOI: 10.1081/DRT-120034267 0737-3937 (Print); 1532-2300 (Online)

in terms of the rate of water content removal, heat transfer, and moisture distribution. Results were compared to those of drying when using convective heat. It is evident that the use of thermal radiation combined with convective heat will help in improving the drying rate. Numerical results show that both the radiative energy absorbed by the solution and the substrate and the distribution of water mass fraction in the solution are closely related to the rate of water removal from the solution during the process.

Key Words: Effective absorption coefficient; Irradiation.

INTRODUCTION

One of the most important physical processes in the coating industry is the loss of volatile materials from the coating layer. It inevitably affects the quality of the products because it is the final process in their manufacture. So, understanding the drying kinetics of a polymer film cast from a polymer/solvent solution is a major issue in numerous industrial processes. Among applications is the drying of paintings, pulp, and paper. During drying simultaneous heat and mass transfers occur inside the particular medium and also in the boundary layer of the drying agent. Drying is one of the most energy-consuming processes in the industrial sector and can also be very time-consuming as in conventional convective drying by hot air, while minimum cost and energy consumption and maximum product quality are among the main concerns in industry today. In convective drying, heat is subjected to the surface and transferred to the internal region by conduction. Longer drying times are typically required, leading to higher energy consumption, higher cost, and lower production line speed. Here, drying time is defined as the required time for a material to dry to the minimum moisture content in the given conditions. In order to optimize the process accomplishment and energy operation, drying by high intensity thermal radiation has been used in a number of fields. In the instance of infrared radiation, due to its strong penetration capacity, the temperature distribution in products will be more uniform compared to convective heat drying, and the quality of products can be improved.[1] Cote et al.[2] showed that the variation of water content, in the case of convective air heating, was small compared to radiation heating. However, the evaporated water can be removed to increase the drying rate. The drying rate here is defined as the amount of water removed from the dried material in unit time per unit of drying surface, i.e., the rate of water content removal. Other benefits of the

Marcel Dekker, Inc.
270 Madison Avenue, New York, New York 10016

application of infrared radiation are as follows: easy and rapid thermal control, clean working environment, and straightforward heat transfer. Fundamental studies related to the application of infrared radiation in drying have caught attention during recent years.

Over the previous decades, many studies have been done analyzing the heat and mass transfer during the drying process using convective heat. Chen and Pei[3] present an elaborate review of the transfer of heat and moisture in porous media by convective heating. They analyzed the mass transfer mechanism during the convective heating process in detail. In terms of the analysis of thermal radiation drying processes, a few works were found. Navarri and Andrieu[4] investigated the drying of a thin wet layer of sand under intensive infrared radiation, showing that drying rates and solid temperature data would be much higher than under conventional convective heating. However, they worked with the assumption that IR radiation was absorbed at the surface of the product. Nishimura et al.[5,6] present an investigation of the radiative heating process. They studied the monochromatic radiative properties of coated films and the moisture redistribution process of an aqueous polymer solution in which the temperature gradients inside the polymer solution and the substrate were neglected. Hashimoto et al.[7] studied the effects of particle properties and the radiative heat source on drying and investigated the factors influencing the drying rate by means of infrared radiation. They also examined the spectral distribution of irradiation power, excluding the variation of the temperature of the drying medium. Previous studies have also simplified drying by infrared radiation by using the lumped-system approximation. Chen and Lin[8] present a radiative drying process of the polymer solution theoretically with the gray assumption; the results were analyzed in terms of the thermal field of the solution layers. In their study, the influence of the radiative properties of a polymer solution on drying was examined in detail. They also checked the validity of the lumped-system assumption in the thermal field during the heat and moisture transfer processes. Fernandez and Howell[9] investigated the radiative drying process of a porous material including both heat and mass transfer based on the fact that the absorption and scattering coefficients of drying materials are spectrally dependent. Infrared drying as an intermittent process both during the active and the tempering stages was studied by Chen and Lin[10] and Tan et al.[11] They showed that a high drying rate can be obtained after the tempering stage and indicate that an intermittent heating process during the tempering stage can reduce net heating time as well as energy consumption. Afzal et al.[12] experimentally investigated the drying process of barley under combined FIR-convection and under convection alone. They found that

Marcel Dekker, Inc.
270 Madison Avenue, New York, New York 10016

the use of infrared radiation enhances the drying rate. Hebbar and Rastogi[13] utilized infrared radiation to dry cashew kernels and measured the variations of the moisture content over time. They also determined the values of effective diffusion coefficients for different temperatures. Lee et al.[14] studied the thermal characteristics of the drying process under two different kinds of radiant sources. A narrow-band emitter caused a smaller temperature gradient inside the films than a grey body emitter. Jun and Irudayaraj[15,16] designed an infrared radiation drying system for the selective heating of food powders. Different incident FIR sources were used by means of band-pass filters because of the selective absorptivity of food components. A simulation model was developed and results compared well with the experimental data. Topic[17] developed three kinds of dryers for the drying of biological materials. He presented the effects of various design parameters that influenced drying characteristics and showed that the radiation source affected the drying rate and material quality. When the moist materials were dried by infrared radiation, the depth of penetration of radiation depended on the properties of the materials and the wavelength of the radiation. In some studies, the drying media whose radiative properties did not vary across the electromagnetic spectrum were considered. The gray assumption in radiative properties is often preferred to the smaller relevant part of the spectrum, in reality this is seldom the case for participating media. It is difficult to realize the accurate solutions for the radiative transfer equation unless the spectral variation of the radiation properties is taken into account. Unfortunately, the consideration of the spectral variations of radiation properties tends to increase the difficulty of an already extremely complicated problem considerably, or at least makes the numerical solution many times more computer-time intensive. It is common practice in engineering to treat properties as constants, which linearizes the problem. Very accurate results can be obtained with such an analysis if an appropriate, constant effective property can be found. Arpaci and Gozum[18] introduced the effective absorption coefficient which is the square root of the product of the Planck and Rosseland means of the absorption coefficient into the radiative transfer equation in order to examine the Benard problem of the radiating nongray fluids. This method performed considerably better with optical thickness ranging in value from 0 to 100.[19]

The objectives of the present study were to establish a mathematical model for extensively simulating the heat and moisture transfer processes of a PVA solution during radiative heating in which combined nongray radiation and conduction heat transfer were involved, while using conduction heat transfer in the substrate. Effective absorption

Marcel Dekker, Inc.
270 Madison Avenue, New York, New York 10016

coefficients were incorporated in the radiative transfer analysis. It was assumed that the diffusion of water in the PVA solution follows Fick's law. The mass diffusion coefficient and equilibrium vapor pressure of water in the PVA solution were assumed to be functions of mass fraction and temperature. The temperature and mass fraction distributions of the PVA solution were computed during the drying process, and the effects of various radiation and convection parameters on heat and mass transports in the solution were then examined. The influence of various spectral distributions of irradiation power on heat and mass transfer in the solution layer were also investigated in terms of drying rate, temperature, and moisture distribution.

MATHEMATICAL MODEL

We present a physical configuration in Fig. 1 for modeling the transfer of heat and mass of polyvinyl alcohol (PVA) solution layer which is exposed to the high intensity infrared radiation and/or an air flow. The origin of the coordinate is fixed at the solution surface. We consider a PVA solution layer on a substrate of finite thickness, in which the lateral variations in composition and temperature are examined. The combined conduction and nongray-radiation heat transfer modes are considered in the PVA solution while the substrate is assumed to be optically thick and thermal radiation interacting with the substrate is only a boundary phenomenon at the interface between solution and substrate. The absorption coefficients in PVA solution are frequency-dependent. The effective absorption coefficients are introduced and incorporated into the radiative transfer analysis. We also include the air flow at specified

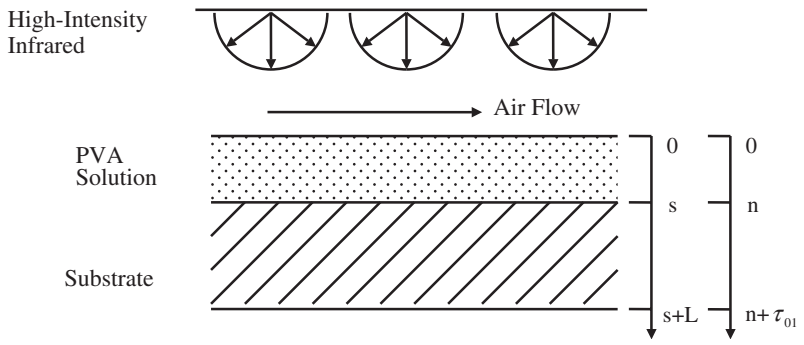

Figure 1. Physical model with geometric and optical coordinates.

MARCEL DEKKER, INC.
270 Madison Avenue, New York, New York 10016

temperature and relative humidity which removes the water evaporated from solution. As no forced air flow is supplied, natural convection would be the mechanism that brings the water vapor out of solution surface. During the drying processes, the main mechanism of moisture transfer is assumed to be the diffusion of water through the PVA and evaporation of water from the surface. And the liquid is driven by the gradient of mass fraction. The diffusion obeys the Fick's second law but mass diffusion coefficient shows strong concentration and temperature dependence.

The governing equations for a one-dimensional transient energy and mass transfer problem can be written as followings in terms of non-dimensional parameters to predict the unsteady temperature of PVA solution and substrate and mass fraction of water. They are, respectively, given as

$$\frac{\partial\theta_1}{\partial\zeta}+\frac{dS}{d\zeta}\frac{\partial\theta_1}{\partial\tau_1}\frac{[n(\zeta)-\tau]}{S}=\frac{\partial}{\partial\tau_1}\left[\left(\frac{\beta_{\text{eff}}}{\beta_0}\right)^2\frac{\alpha_{\text{eff}}}{\alpha_2}\frac{\partial\theta_1}{\partial\tau_1}\right]-\left(\frac{\beta_{\text{eff}}}{\beta_0}\frac{\alpha_{\text{eff}}}{\alpha_2}\frac{k_2}{k_{\text{eff}}}\right)\times\frac{1}{N}\frac{\partial Q^r}{\partial\tau_1},\quad 0<\tau_1<n(\zeta) \tag{1}$$

$$\frac{\partial\theta_2}{\partial\zeta}=\frac{\partial^2\theta_2}{\partial\tau_2^2},\quad n(\zeta)<\tau_2<n(\zeta)+\tau_{02} \tag{2}$$

$$\frac{\partial y}{\partial\zeta}+\frac{dS}{d\zeta}\frac{\partial y}{\partial\tau_1}\frac{[n(\zeta)-\tau_1]}{S}+\frac{2\bar{D}}{y+\hat{y}}\left(\frac{\beta_{\text{eff}}}{\beta_0}\frac{\partial y}{\partial\tau_1}\right)^2=\frac{\partial}{\partial\tau_1}\left[\left(\frac{\beta_{\text{eff}}}{\beta_0}\right)^2\bar{D}\frac{\partial y}{\partial\tau_1}\right],\quad 0<\tau_1<n(\zeta) \tag{3}$$

where $dS/d\zeta$ represents the dimensionless drying rate which can be then obtained as

$$R=-\frac{dS}{d\zeta}=-\frac{h_m(P_a-P)}{\alpha_2\beta_0^2 s_0 \overset{\circ}{\rho}_A} \tag{4}$$

The second term on the left hand side of Eqs. (1) and (3) exists due to the moving of boundary. α_{eff} and k_{eff} are the effective thermal diffusivity and conductivity of the solution layer, respectively. The solution medium is considered to be radiatively absorbing and emitting and nongray. The variation of the optical thickness depends on the composition of

Marcel Dekker, Inc.
270 Madison Avenue, New York, New York 10016

the solution. The relationship between geometric thickness, s, and optical thickness of solution layer, $n(\zeta)$, is given as

$$n(\zeta) = \left(s - \frac{\rho_{B0} s_0}{\overset{\circ}{\rho}_B}\right)\beta_{\text{eff},A} + \frac{\rho_{B0} s_0}{\overset{\circ}{\rho}_B}\beta_{\text{eff},B} \tag{5}$$

$\beta_{\text{eff},A}$ and $\beta_{\text{eff},B}$ are the effective absorption coefficient of water and PVA, respectively. They can be written as[18]

$$\beta_{\text{eff},A} = \sqrt{\beta_{P,A}\beta_{R,A}} \quad \text{and} \quad \beta_{\text{eff},B} = \sqrt{\beta_{P,B}\beta_{R,B}} \tag{6}$$

where β_P is the Planck-mean absorption coefficient and β_R is the Rosseland-mean absorption coefficient.[20] The effective absorption coefficient of solution, β_{eff}, is expressed as

$$\beta_{\text{eff}} = (1 - \frac{\rho_{B0} s_0}{\overset{\circ}{\rho}_B s})\beta_{\text{eff},A} + \frac{\rho_{B0} s_0}{\overset{\circ}{\rho}_B s}\beta_{\text{eff},B} \tag{7}$$

β_0 in Eqs. (1) and (3) is the initial absorption coefficient.

For the PVA solution, the effective absorption coefficient is large. And thus the effect of radiation emission then cannot be negligible even while the temperature of solution is low. The radiation contribution in Eq. (1) can be expressed as

$$\frac{\partial Q^r}{\partial \tau} = \left(\frac{\beta_{\text{eff},e}}{\beta_{\text{eff}}}\theta_1^4 - G^*\right), \quad 0 < \tau_1 < n(\zeta) \tag{8}$$

with nondimensional incident radiation G^* being obtained from the following transfer equation of radiation. $\beta_{\text{eff},e}$ is known as the effective absorption coefficient of solution for emission.[19]

In the present model, we assume that water evaporation takes place only at the surface and the bottom of substrate is adiabatic. The initial and boundary conditions for energy equations are thus as follows:

$$\theta_1 = \theta_2 = \theta_0 \quad \text{at } \zeta = 0 \tag{9}$$

$$-\frac{k_{\text{eff}}}{k_2}\frac{\beta_{\text{eff}}}{\beta_0}\frac{\partial \theta_1}{\partial \tau_1} = \frac{\overset{\circ}{\rho}_A}{\rho_2}\frac{n(0)}{\text{Ja}}\frac{dS}{d\zeta} - \text{Bi}(\theta_1 - \theta_\infty) \quad \text{at } \tau_1 = 0 \tag{10}$$

$$\frac{\partial \theta_1}{\partial \tau} + \frac{Q^r}{N} = \frac{k_{\text{eff}}}{k_s}\frac{\partial \theta_2}{\partial \tau} \quad \text{and } \theta_1 = \theta_2 \text{ at } \tau = n(\zeta) \tag{11}$$

$$\frac{\partial \theta_2}{\partial \tau_2} = 0 \quad \text{at } \tau_2 = n(\zeta) + \tau_{02} \tag{12}$$

Marcel Dekker, Inc.
270 Madison Avenue, New York, New York 10016

where Ja is the Jakob number which is the ratio of sensible to latent energy absorbed during liquid–vapor phase change and Bi is the Biot number. They can be expressed as

$$\mathrm{Ja} = \frac{c_{p2} T_r}{\gamma_A} \quad \text{and} \quad \mathrm{Bi} = \frac{h}{k_2 \beta_0}$$

γ_A in the expression is the latent heat of water at evaporation temperature. h is the convective heat transfer coefficient.

The transfer equation of radiation is expressed as

$$\mu \frac{\partial \psi(\tau_1, \mu)}{\partial \tau_1} + \psi(\tau_1, \mu) = \frac{\beta_{\mathrm{eff},e}}{\beta_{\mathrm{eff}}} \psi_b(\tau_1), \quad 0 < \tau_1 < n(\zeta), \ -1 \le \mu \le 1 \tag{13}$$

The nondimensional incident radiation can be expressed in terms of the nondimensional radiation intensity $\psi(\tau_1, \mu)$ as

$$G^* = \frac{1}{2} \int_{-1}^{1} \psi(\tau_1, \mu) d\mu, \quad 0 < \tau_1 < n(\zeta) \tag{14}$$

Since the diffuse incidence of thermal radiation upon the semitransparent boundary of solution layer is considered and at the interface between the substrate and PVA solution the substrate may emit, absorb, and reflect thermal radiation, the radiation boundary conditions are expressed as

$$\psi(0, \mu) = \frac{(1 - \rho_1'^d) Q_{\mathrm{in}}}{\pi} + 2\rho_1^d \int_0^1 \psi(0, -\mu') \mu' d\mu' \tag{15}$$

and

$$\psi[n(\zeta), -\mu] = \varepsilon_2 \theta_1 [n(\zeta)]^4 + 2\rho_2^d \int_0^1 \psi[n(\zeta), \mu'] \mu' d\mu', \quad 0 \le \mu \le 1 \tag{16}$$

where $\rho_1'^d$ and ρ_1^d are respectively the external and internal hemispherical reflectivities of the air–solution interface. ρ_2^d is the hemispherical reflectivity of the solution–substrate interface. They all are total, hemispherical reflectivities and calculated from Fresnel's equations. ε_2 is total, hemispherical emissivity.

Under the assumption that the substrate is impermeable, the corresponding initial and boundary conditions for mass transfer

equation are

$$y = 1 \quad \text{at } \zeta = 0 \tag{17}$$

$$\bar{D}\frac{\partial y}{\partial \tau} = \frac{h_m(P - P_a)(y + \hat{y})}{\hat{\omega}^2 \overset{\circ}{\rho}_A \overset{\circ}{\rho}_B \alpha_2 \beta_{\text{eff}}} \times \left[\{(\omega_{A0} - \omega_{Ae})y + \omega_{Ae}\}(\overset{\circ}{\rho}_A - \overset{\circ}{\rho}_B\hat{\omega}) + \overset{\circ}{\rho}_A\hat{\omega}\right] \quad \text{at } \tau_1 = 0 \tag{18}$$

and

$$\frac{\partial y}{\partial \tau_1} = 0 \quad \text{at } \tau = n(\zeta), \tag{19}$$

where h_m is the convective mass transfer coefficient. Both the dimensionless mass diffusion coefficient, $\bar{D}$, and vapor pressure of water at the surface, P, are strongly dependent of temperature and moisture mass fraction in solution[21] and $\bar{D}$ increases with temperature following an Arrhenius law and

$$P = P_{s,T} \times a(\omega_A) \tag{20}$$

with $P_{s,T}$ being the saturated pressure of water vapor at temperature T(K),[22] and $a(\omega_A)$ is the activity at the concentration of ω_A. P_a is partial pressure of water vapor in air. It can be represented as

$$P_a = \frac{\omega_H P_\infty}{(\omega_H + 0.622)}, \tag{21}$$

where ω_H is humidity ratio, and P_∞ is atmospheric pressure.

NUMERICAL METHODOLOGY

The numerical technique employed to solve the set of nonlinear energy and mass transfer equations is the fully implicit time discretization scheme which is used in order to allow for larger time steps. Linearization is accomplished by evaluating the nonlinear coefficients at the previous time step. The central difference for the spatial derivatives in these equations is used. To deal with the moving boundary problem, we use the time-dependent coordinate systems[23] i.e., the variable grid space at fixed grid number is utilized to numerically solve the system of partial differential equations. The time derivative term in the transformed plane can be shown as:

$$\left.\frac{\partial u}{\partial t}\right|_{\text{physical}} = \left.\frac{\partial u}{\partial t}\right|_{\text{transformed}} + \frac{dx}{dt}\frac{\partial u}{\partial x} \tag{22}$$

Marcel Dekker, Inc.
270 Madison Avenue, New York, New York 10016

Note that in the transformed expression for the time derivatives, all derivatives are taken at the fixed grid points in the transformed plane. The movement of the grid in the physical plane is reflected only through the rates of change of x at the fixed grid points in the transformed plane.

The fractional functions had been utilized associated with the consideration of the Planck-mean absorption coefficient and the Rosseland-mean absorption coefficient. Suppose that the entire wavelength spectrum is divided into M wavelength bands such that over each band the value of β_λ can be approximated as constant. Then the Planck-mean absorption coefficient β_P can be represented as a summation, and we obtain

$$\beta_P = \sum_{m=1}^{M} \beta_{\lambda_m} \left[f_{0-\lambda_m}(T) - f_{0-\lambda_{m-1}}(T) \right] \tag{23}$$

where β_{λ_m} is the mean value of β_λ in the wavelength interval from λ_{m-1} to λ_m. $f_{0-\lambda}(T)$, the fraction of the total black-body radiation intensity having wavelength between 0 and λ, is called the fractional function of the first kind. The Rosseland-mean absorption coefficient can be written in the form

$$\frac{1}{\beta_R} = \sum_{m=1}^{M} \frac{1}{\beta_{\lambda_m}} \left[f^*_{0-\lambda_m}(T) - f^*_{0-\lambda_{m-1}}(T) \right] \tag{24}$$

where $f^*_{0-\lambda}(T)$ is called the fractional function of the second kind. It is interesting to note that the mean absorption coefficient depends on the spectral absorption coefficient and on temperature. The temperature of the radiation source is used for calculation while the mean absorption coefficient is required for absorption, and the temperature of medium is used for emission. Then the spectral absorption coefficients of water[24] and PVA[25] are used to obtain the effective absorption coefficients which are the square root of the product of the Planck and Rosseland means of the absorption coefficients and are shown in Fig. 2.

The radiation contribution is solved by the P3 approximation technique[20] since it is difficult to obtain the exact solution of radiation distribution. The nondimensional intensity of radiation is represented as

$$\psi(\tau_1, \mu) = \sum_{m=0}^{3} \frac{2m+1}{4} P_m(\mu) \varphi_m(\tau_1) \tag{25}$$

Substitution of Eq. (25) into the radiative transfer equation, Eq. (13), results in four sets of ordinary differential equations for the functions

Marcel Dekker, Inc.
270 Madison Avenue, New York, New York 10016

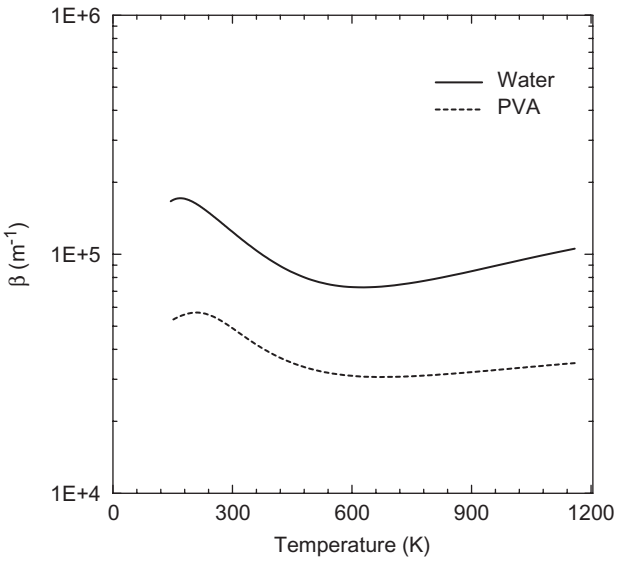

Figure 2. Effective absorption coefficients of PVA and water.

$\phi_m(\tau_1)$. To solve the four equations, we utilize the Marshak's boundary conditions to approximate the radiative boundary conditions for the P3 scheme. By applying the orthogonality of the Legendre polynomials $P_m(\mu)$, we obtain that $G^*(\tau_1) = \phi_0(\tau_1)/4\pi$ and $Q^r(\tau_1) = \phi_1(\tau_1)/4\pi$.

Since the nonlinear energy and mass transfer equations with moving boundary effect are solved, the alternating under-relaxation factor for temperature and mass fraction is employed in the iterative procedure to quicken the convergence of the solutions. At each time increment, the nodal values of temperature and mass fraction are solved iteratively and convergence is checked on both variables. Combined with the boundary conditions, the Gauss elimination method is employed to solve for the variables at a new time level. If the convergent solution is not attained, the newly calculated variables are used to update the parameters for next iteration. The procedure continues until convergence is found according to a prescribed condition (the maximum relative errors of both mass fraction and temperature are under 10^{-3} in the present study). And this procedure is carried out repeatedly along the time axis. In the present study, the grid systems have 401 grid points respectively in the polymer solution and in the substrate and these grids have been checked to ensure grid-independent results.

RESULTS AND DISCUSSION

In what follows, the transfer of heat and moisture in PVA solutions on a substrate, exposed to radiative heating at various convection and radiation parameters, is shown. The nondimensional initial temperature of the PVA solution and substrate are 1.0, i.e., at the temperature of the environment. Using Fresnel's equations, the internal and external reflectivities of the air–solution interface and the reflectivity of the substrate were found. $\rho_1' d$ was taken as 0.094 and ρ_1^d as 0.448 by averaging the directional reflectivity and then integrating it spectrally. Aluminum, silver, and stainless steel plates were used as the substrates. The monochromatic emissivities of these plates were used,[7] to obtain the total hemispherical emissivity which is the spectral average with the spectral emissive power as weight factor. ε_2 for the aluminum plate was taken as 0.503, for the silver plate as 0.189 and for the stainless steel plate as 0.018 with the temperature range from 300 to 370 K. The composition of the solution varied during the moisture transfer, and consequently the complex refractive index of the solution varied. The physical properties for different compositions were weighted in proportion to the composition. The real part of the refractive index of solution was between 1.33 and 1.5, since that of the water was 1.33 and the PVA about 1.5.[25] The absorption coefficients of the water and PVA, ranging from 10^3 to $10^7\,\mathrm{m}^{-1}$ for radiation wavelength 2 μm through 22 μm, were related to the imaginary part of the refractive index of the water and PVA through $\beta = 4\pi\kappa/\lambda$, where κ is the imaginary part of the refractive index. The mean temperature of medium, about 60°C, was used for calculation while the effective absorption coefficient was required for emission. The thermal conductivity of the substrate of the aluminum, silver, and stainless steel plates, water and PVA used here were 204, 407, 54, 0.604, and $0.169\,\mathrm{W\,m^{-1}\,K^{-1}}$,[26] respectively. In the numerical calculations, heat transfer coefficient, h, of $30\,\mathrm{W\,m^{-2}\,K^{-1}}$, corresponding to the application of air flow with a parallel speed of $2.5\,\mathrm{m\,s^{-1}}$, and convective mass transfer coefficient, h_m, of $1.7 \times 10^{-7}\,\mathrm{kg\,m^{-2}\,s^{-1}\,Pa^{-1}}$[21] were used. When no forced convection air flow was applied, natural convection was included and h of $6.5\,\mathrm{W\,m^{-2}\,K^{-1}}$[26] and h_m obtained by an analogical relationship (i.e., $3.81 \times 10^{-8}\,\mathrm{kg\,m^{-2}\,s^{-1}\,Pa^{-1}}$) were utilized.[27] The humidity ratio of the ambient air, ω_H, was taken to be 0.0047. The initial thickness of the solution layer, s_0, was 2.5×10^{-4} m with initial water mass fraction, ω_{A0}, equal to 0.95 by weight. In the following, the influence of the various convection and radiation parameters on heat and mass transfer processes is examined. The parameters of above values are used unless otherwise specified.

Marcel Dekker, Inc.
270 Madison Avenue, New York, New York 10016

The influence of different types of heating, including combined convective and radiative heating and pure radiative heating, on transient moisture and heat transfer processes at $Q_{in} = 0.5$, $n(0) = 18.26$ and various ambient air temperatures, θ_{out}, were plotted and were shown in Figs. 3 and 4. Bi, equal to 6.67×10^{-5}, was utilized, corresponding to the heat transfer by natural convection. Figure 3 shows the variations of the percentage of residual weight compared to the initial weight of the polymer solution, W, the surface temperature of polymer solution, θ_s, and the drying rate, R, with respect to time. The predicted water mass fraction distributions at various times within the polymer solution are also presented in Fig. 4. Because of the evaporation of water, the boundary was moving and the thickness of the polymer solution changed. d in the figure represents the location normalized to the thickness of the solution layer with the solution surface located at $d = 0$. Regarding the drying mechanism in the combined radiative and convective heating process with higher θ_{out}, it was clear that, when the external mass transfer for water vapor and radiative heat input were applied, the drying rate increased initially. The temperature of the solution also increased since the required latent heat was not so high and part of the energy input was

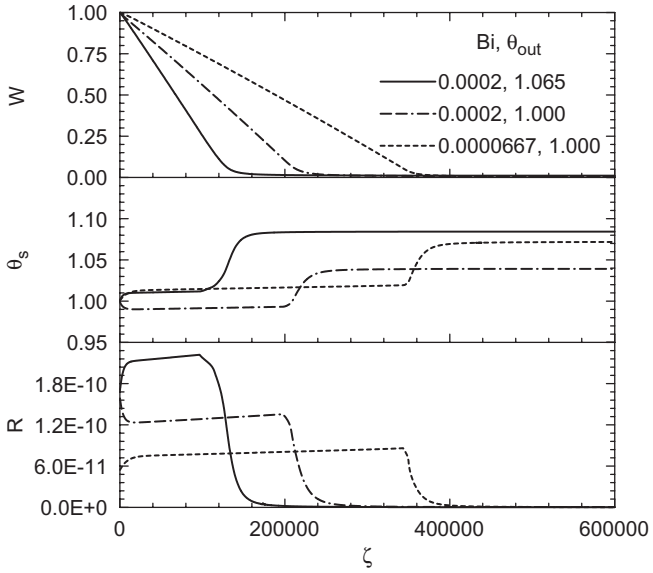

Figure 3. Variations of solution weight, surface temperature, and drying rate with respect to time at various heating.

Marcel Dekker, Inc.
270 Madison Avenue, New York, New York 10016

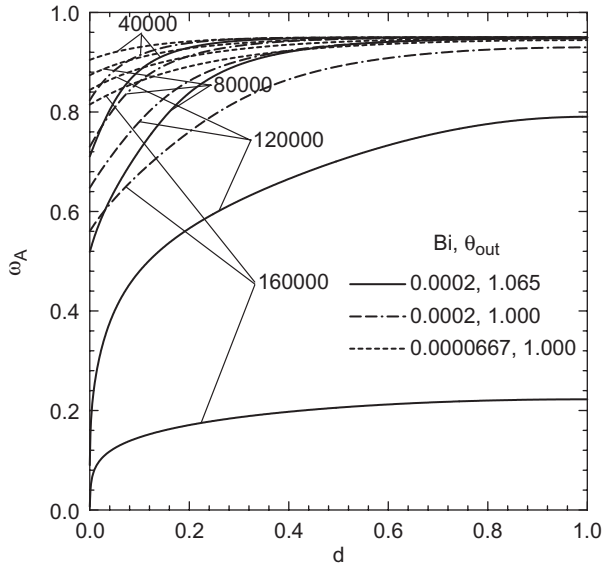

Figure 4. Water content distributions at various times for various heating.

to increase the sensible heat. After this early drying process θ_s reached an equilibrium temperature because the moisture of the product was abundant near the surface and the energy input was balanced by the evaporation of water. It was also found that the moisture removal stayed at a nearly constant rate because the partial pressure difference of water vapor between surface and ambient air was almost constant. Although the water mass fraction at the surface decreased, it was still high. The variation of the water content was independent of the distribution of the water mass fraction in the polymer solution and was controlled by the convection and radiation parameters. This was the so-called constant rate period. The diffusion coefficient in the solution was larger at a higher temperature and a higher water concentration. The higher mass diffusion coefficient was in the interior region of the polymer solution, because more water could diffuse from the interior region to the surface. The activity was also dependent on surface water mass fraction. As the activity was large, the vapor pressure difference between the solution surface and the ambient air was large and consequently the rate of water removal was large. After the constant rate period, the surface water mass fraction continued to drop since the water density near the internal region was transported to the surface at a lower rate than that at which

evaporation occurred, leading to a lower drying rate. During this period, the rate of water removal was strongly related to the water mass fraction profile in the polymer solution. Thus while the drying rate decreased, the temperature increased rapidly. Due to a higher temperature in the polymer solution, the solution emitted more radiative energy to the ambient air while less radiative energy was absorbed in the polymer solution and the substrate. This was the so-called falling rate period. It was found that the convection combined with the radiation drying of the PVA solution showed a higher drying speed than pure radiation drying. It was also found that the required drying time was less at a higher ambient air temperature when using combined modes of heating. While the air temperature was lower, the convective effect did not only carry the water vapor away from the solution surface but also served as a heat sink.

Figures 5 and 6 illustrate the results for the PVA solution exposed to various radiant heat inputs at $\mathrm{Bi} = 2 \times 10^{-4}$ and $n(0) = 18.26$. When the absorption of radiative energy by the PVA solution and substrate was high, the temperature would increase faster, while the drying rate would increase more at the early stages of the drying process. When the surface water content decreased, the drying rate dropped while the temperature

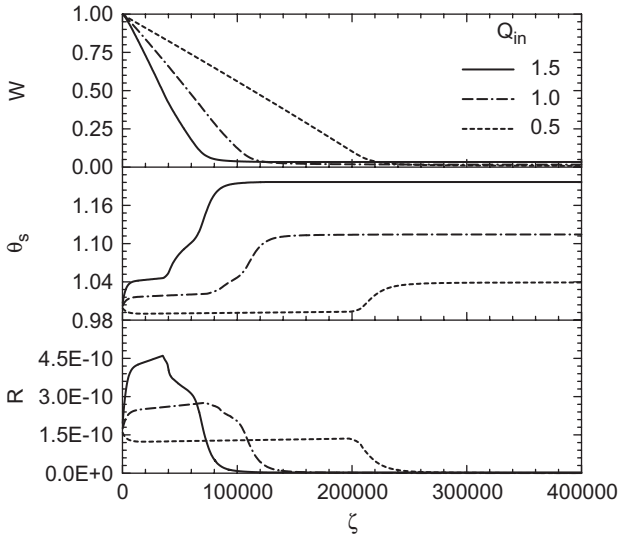

Figure 5. Variations of solution weight, surface temperature, and drying rate with respect to time at various radiative energy input.

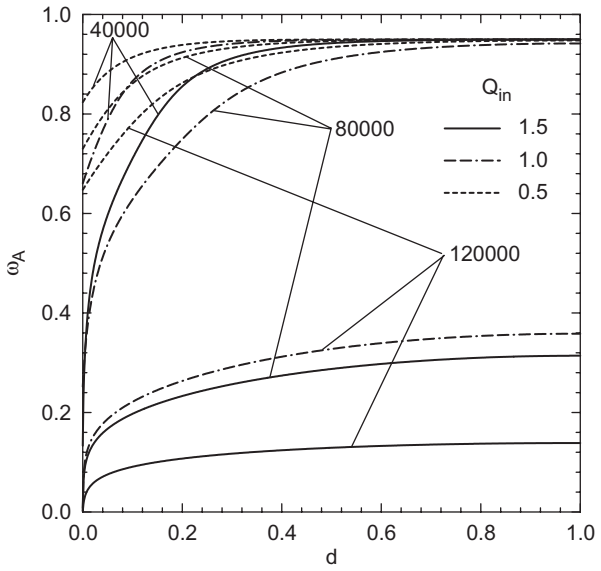

Figure 6. Water content distributions at various times for various radiative energy input.

of the solution still increased. Since the internal temperature of the PVA solution was much higher for the larger Q_{in}, the diffusion of water from the interior region would enhance the drying rate during the latter half of the process. The drying speed was also faster for the larger radiant energy input. The effects of the reflectivity, ρ_2^d, at the interface between solution and substrate on the drying at $Q_{in} = 0.5$ were also examined, but were not shown. The radiation flux would be either absorbed and/or reflected when reaching the interface. Since the optical thickness was huge for all cases at the beginning of the drying, the absorption of radiant energy was basically a surface phenomenon and thus the drying rate and solution temperature were also similar during this period. After that, the optical thickness of the solution decreased to a value at which the effect of radiation reflection and absorption at the interface became significant. As ρ_2^d was not zero, the radiation penetration was reflected at the interface and the absorbed radiant energy decreased at the early stages of the drying. The final temperature of the solution at the lowest ρ_2^d was the lowest. However, the discrepancy in drying rate was not significant.

The effect of various external convective heating conditions on drying characteristics at $Q_{in} = 0.5$ and $n(0)$ as 18.26 can be seen in Figs. 7 and 8.

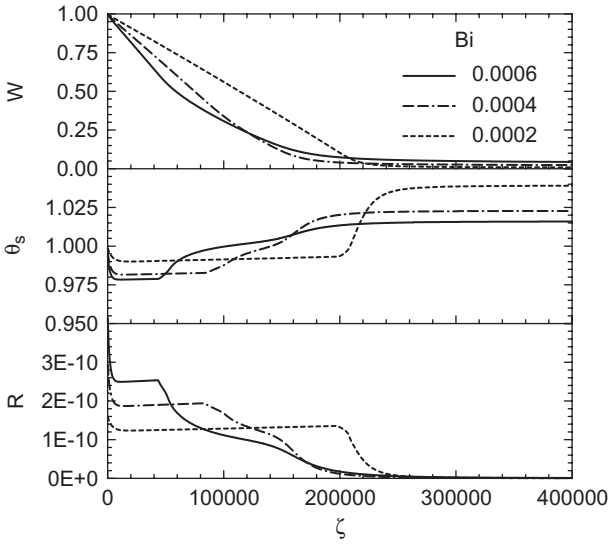

Figure 7. Variations of solution weight, surface temperature, and drying rate with respect to time at various Biot numbers.

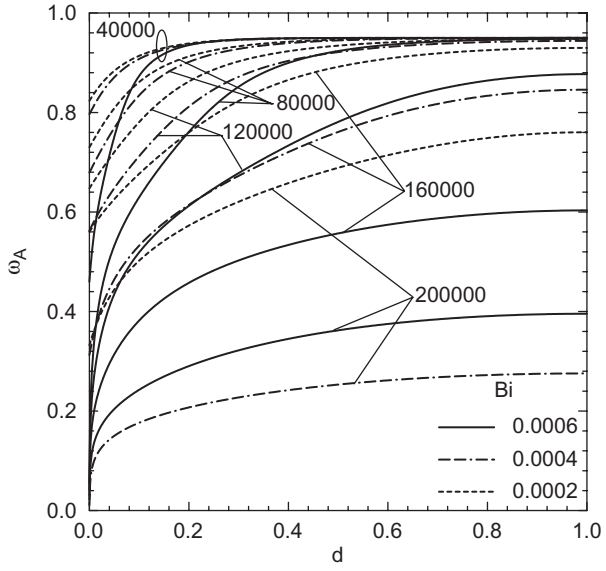

Figure 8. Water content distributions at various times for various Biot number.

Marcel Dekker, Inc.
270 Madison Avenue, New York, New York 10016

The corresponding Bi were 2×10^{-4}, 4×10^{-4}, and 6×10^{-4}, and the mass transfer coefficients, h_m, were 1.13×10^{-7}, 2.27×10^{-7}, and $3.4 \times 10^{-7}\,\mathrm{kg\,m^{-2}\,s^{-1}\,Pa^{-1}}$, respectively. In regard to the drying of the PVA solution, it was clear that while the external mass transfer of the water vapor was happening, the drying rate increased initially. For the higher Bi the drying rate reached the maximum since the external transfer coefficient was larger it decreased because of insufficient energy input, while the surface temperature slightly decreased since more latent heat was required. When Bi was smaller the drying rate and temperature of the solution increased since the required latent heat was not so high. It was also observed that during the early drying period, the water content at the surface was higher. The water evaporating rate from the PVA solution was independent of the distribution of water content, and the drying rate was controlled by the external heating conditions. This occurred in the constant rate period. The surface water content continued to drop since there was less water density near the surface, leading to a lower drying rate because of the effect of the activity coefficient. During the constant rate period, the drying rate was higher. It was also found that the water content near the surface decreased more with the higher Bi. After the constant rate period, the drying rate dropped and the temperature increased rapidly. Since the activity coefficient was a function of the surface water content and the drying rate was dominated by the diffusion of water, the higher mass diffusion coefficient was in the PVA solution, and more water could diffuse from the interior region to the surface. The drying rate was higher while the activity coefficient was large. In the case of the high Bi, the diffusion in the PVA solution was small due to lower temperature distribution and the effect of high external mass transfer reduced the surface water content. The drying rate decreased much more for the higher Bi. More time was thus required to obtain complete drying. Therefore, higher external convective heating may not improve drying speed.

Figures 9 and 10 present the results for the various values of the absorption coefficient β_{eff} at $Q_{\mathrm{in}} = 0.5$ and $\mathrm{Bi} = 2 \times 10^{-4}$. In Fig. 9 Q_{abs} is the absorbed radiative heat flux in the PVA solution and substrate. Here, different values of absorption coefficients were used corresponding to different sources of infrared heating. Three infrared heaters, behaving like blackbodies at 1449, 724.5, and 362.25 K, were utilized, i.e., the radiative emission of the heaters respectively corresponded to the peak wavelength at 2, 4, and 8 μm. The solution medium was considered to be radiatively absorbing, emitting and nongray. As the optical thickness was huge for the larger absorption coefficient during the beginning of the drying, the absorption of radiant energy was basically a surface

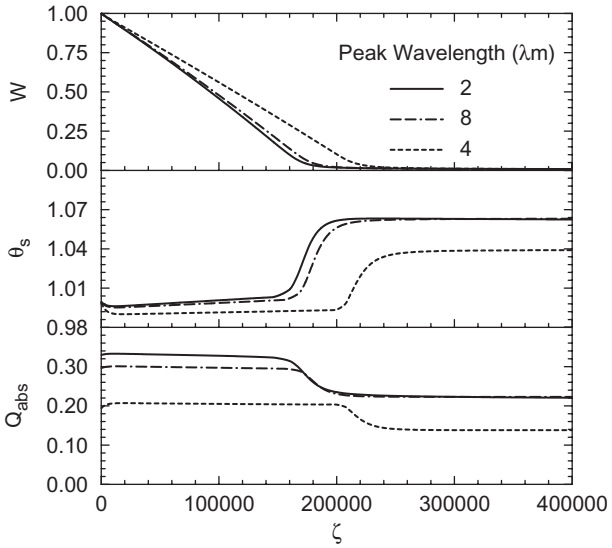

Figure 9. Variations of solution weight, surface temperature, and drying rate with respect to time at various spectral distribution of irradiation power.

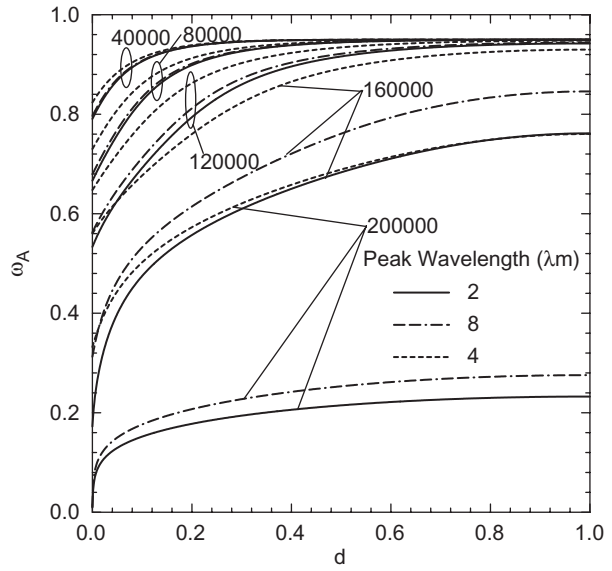

Figure 10. Water content distributions at various times for various spectral distribution of irradiation power.

Marcel Dekker, Inc.
270 Madison Avenue, New York, New York 10016

phenomenon. However, the ratios of the initial effective absorption coefficient of the solution for emission to the initial effective absorption coefficient of the solution for absorption, $\beta_r (= \beta_{\text{eff},e}/\beta_{\text{eff}})$, are 0.984, 1.122, and 1.545 for 2, 8, and 4 μm, respectively. The effective absorption coefficient of the solution for absorption corresponding to the peak wavelength at 2 μm was larger than that corresponding to the other two because of the strong absorption band near 3 μm. In the solution medium, the emitted radiation was greater than the amount of absorbed radiation while β_r was greater than 1.0. The temperature of the solution decreased initially since the emission effect served as a heat sink, and then it reached an equilibrium temperature. The absorbed radiative heat flux in the solution and substrate was lower when β_r was greater, and consequently, the temperature of the medium was lower. The energy supplied for the evaporation of water on the solution surface was smaller at larger β_r. Thus the required drying time would be longer.

CONCLUSION

In our study, the heat and mass transfer processes of a PVA solution that was exposed to the high-intensity nongray irradiation and/or air flow were theoretically investigated. Effective absorption coefficients were incorporated in the radiative transfer analysis. It is evident that radiation drying combined with the use of convective hot air results in a higher drying rate than pure infrared heat drying. The effects of various radiation and convection parameters on the heat and mass transfer processes were also examined. Results show that the net amount of radiant energy absorbed by the solution layer and the substrate has significant effects on the thermal field. Also, that the rate of water removal is closely related not only to the absorbed radiative energy, but also to the moisture distribution in the polymer solution. It is clear that the drying rate is higher with higher radiant energy absorption and larger moisture mass fraction near the surface.

NOMENCLATURE

d	Location normalized to the thickness of polymer solution $(= x/s)$
$\bar{D}$	Dimensionless mass diffusion coefficient $(= D/\alpha_2)$
N	Conduction to radiation parameter $(= k_2\beta_0/4\sigma T_0^3)$

Marcel Dekker, Inc.
270 Madison Avenue, New York, New York 10016

Q_{in}, Q^r	Dimensionless radiative energy input and flux, respectively ($= q_{in}/4\sigma T_0^4,\ q^r/4\sigma T_0^4$)
R	Dimensionless drying rate
S	Dimensionless geometric thickness of solution layer ($= s/s_0$)
$y, \hat{y}$	Dimensionless mass fractions of water [$=(\omega_A - \omega_{Ae})/(\omega_{A0} - \omega_{Ae}),\ (\hat{\omega} - \omega_{Ae})/(\omega_{A0} - \omega_{Ae})$]

Greek Symbols

α	Thermal diffusivity ($= k/\rho c_p$)
ε_2	Emissivity at the surface of substrate
θ	Dimensionless temperature ($= T/T_0$)
$\overset{\circ}{\rho}$	Density
ρ^d	Diffuse reflectivity
τ_1, τ_2	Optical distance ($= \beta_{\text{eff}}x, \beta_{\text{eff}}x$)
ω	Mass fraction
ψ	Dimensionless radiative intensity ($= \pi I/\sigma T_0^4$)
ζ	Dimensionless time ($= \alpha_2\beta_0^2 t$)

Subscripts

0	Initial value
1	Polymer solution
2	Substrate
A	Water
B	Polymer

REFERENCES

1. Stephansen, E.W. New high-intensity infrared radiation reduces binder migration on coating. TAPPI Journal **1986**, *69*, 42–44.
2. Cote, B.; Broadbent, A.D.; Therien, N. Modeling and simulating continuous drying of thin-layers by infrared radiation. The Canadian Journal of Chemical Engineering **1990**, *68*, 786–794.
3. Chen, P.; Pei, D.C.T. A mathematical model of drying processes. International Journal of Heat and Mass Transfer **1989**, *32*, 297–310.

Marcel Dekker, Inc.
270 Madison Avenue, New York, New York 10016

4. Navarri, P.; Andrieu, J. High-intensity infrared drying study part I. Case of capillary-porous material. Chemical Engineering Processes **1993**, *32*, 311–318.
5. Nishimura, M.; Kuraishi, M.; Bando, Y. Effect of internal heating on infrared drying of coated films. Kagaku Kogaku Ronbunshu **1983**, *9*, 148–153.
6. Nishimura, M.; Kuraishi, M.; Bando, Y.; Kojima, H. Influence of the spectral distribution of incident radiation on the effect of internal heating in infrared drying of coated films. Kagaku Kogaku Ronbunshu **1984**, *10*, 124–126.
7. Hashimoto, A.; Yamazaki, Y.; Shimizu, M.; Oshita, S. Drying characteristics of gelatinous materials irradiated by infrared radiation. Drying Technology **1994**, *12* (5), 1029–1052.
8. Chen, J.J.; Lin, J.D. Analysis of heat and mass transfer in drying processes of polymer solution using high-intensity infrared radiation. In *Drying '96*; Mujumdar, A.S, Ed.; Lodz Technical University: Poland, 1996; 93–102.
9. Fernandez, M.L.; Howell, J.R. Radiative drying model of porous materials. Drying Technology **1997**, *15* (10), 2377–2399.
10. Chen, J.J.; Lin, J.D. Simultaneous heat and mass transfer in polymer solutions exposed to intermittent infrared radiation Heating. Numerical heat Transfer, Part A **1998**, *33*, 851–873.
11. Tan, M.; Chua, K.J.; Mujumdar, A.S.; Chou, S.K. Effect of osmotic pre-treatment and infrared radiation on drying rate and color changes during drying of potato and pineapple. Drying Technology **2001**, *19* (9), 2193–2207.
12. Afzal, T.M.; Abe, T.; Hikida, Y. Energy and quality aspects during combined FIR-convection drying of barley. Journal of Food Engineering **1999**, *42*, 177–182.
13. Hebbar, H.U.; Rastogi, N.K. Mass transfer during infrared drying of cashew kernel. Journal of Food Engineering **2001**, *47*, 1–5.
14. Lee, H.; Speyer, R.F.; Patterson, T. Temperature uniformity in water films and wet paper through spectrally selective infrared heating. Drying Technology **2003**, *21* (1), 35–50.
15. Jun, S.; Irudayaraj, J. Selective far infrared heating system-design and evaluation I. Drying Technology **2003a**, *21* (1), 51–67.
16. Jun, S.; Irudayaraj, J. Selective far infrared heating system-spectral manipulation. II. Drying Technology **2003b**, *21* (1), 69–82.
17. Topic, R.M. Small capacity mobile dryers for drying biological materials. Drying Technology **2003**, *21* (6), 1137–1150.
18. Arpaci, V.S.; Gozum, D. Thermal stability of radiating fluids: the Benard problem. The Physics of Fluids **1973**, *16* (5), 581–588.

Marcel Dekker, Inc.
270 Madison Avenue, New York, New York 10016

19. Modest, M.F. *Radiative Heat Transfer*; McGraw-Hill: New York, 1993.
20. Ozisik, M.N. *Radiative Transfer*; Wiley: New York.
21. Okazaki, M.; Shioda, K.; Masuda, K.; Toei, R. Drying mechanism of coated film of polymer solution. Journal of Chemical Engineering of Japan **1974**, *7* (2), 99–105.
22. Haber, S.; Shavit, A.; Dayan, J. The effect of heat convection on drying of porous semi-infinite space. International Journal of Heat and Mass Transfer **1984**, *27*, 2347–2353.
23. Thompson, J.F.; Thames, F.C.; Mastin, C.W. Automatic numerical generation of body-fitted curvilinear coordinate system for field containing any number of arbitrary two-dimensional bodies. Journal of Computational Physics **1974**, *15*, 299–319.
24. Hale, G.M.; Querry, M.R. Optical constants of water in the 200 nm to 200 μm wavelength region. Applied Optics **1973**, *12*, 555–563.
25. Chen, J.J.; Lin, J.D.; Sheu, L.J. Simultaneous measurement of radiative properties and thickness of an absorbing thin film on a substrate with infrared radiant incidence. Thin Solid Films **1999**, *354*, 176–186.
26. Holman, J.P. In *Heat Transfer*; Metric, S.I., Ed.; McGraw-Hill: New York, 1989.
27. Savoye, I.; Trystram, G.; Duquenoy, A.; Brunet, P.; Marchin, F. Heat and mass transfer dynamic modeling of an indirect biscuit baking tunnel-oven. Part I: modeling principles. Journal of Food Engineering **1992**, *16*, 173–196.

Marcel Dekker, Inc.
270 Madison Avenue, New York, New York 10016